Materials Science and Technology

ISSN: 0267-0836 (Print) 1743-2847 (Online) Journal homepage: https://www.tandfonline.com/loi/ymst20

Ni–Cr–Al Alloy for neutron scattering at high pressures

Yao Cheng, Janik Brenk, Bernd Friedrich, Jörg Perßon, Nour Maraytta, James S. K.-L. Gibson, Sandra Korte-Kerzel, Georg Roth, Yixi Su, Fengfeng Zhu, Carsten Paulmann & Andrzej Grzechnik

To cite this article: Yao Cheng, Janik Brenk, Bernd Friedrich, Jörg Perßon, Nour Maraytta, James S. K.-L. Gibson, Sandra Korte-Kerzel, Georg Roth, Yixi Su, Fengfeng Zhu, Carsten Paulmann & Andrzej Grzechnik (2019): Ni–Cr–Al Alloy for neutron scattering at high pressures, Materials Science and Technology, DOI: 10.1080/02670836.2019.1578077

To link to this article: https://doi.org/10.1080/02670836.2019.1578077

Published online: 13 Feb 2019.

MATERIALS SCIENCE AND TECHNOLOGY
https://doi.org/10.1080/02670836.2019.1578077

The Institute of Materials, Minerals and Mining

Taylor & Francis
Taylor & Francis Group

Ni–Cr–Al Alloy for neutron scattering at high pressures

Yao Cheng[a], Janik Brenk[b], Bernd Friedrich [b], Jörg Perßon [c], Nour Maraytta[c], James S. K.-L. Gibson [d], Sandra Korte-Kerzel[d], Georg Roth[a], Yixi Su[e], Fengfeng Zhu[e], Carsten Paulmann[f] and Andrzej Grzechnik[a]

[a]Institute of Crystallography, RWTH Aachen University, Aachen, Germany; [b]IME Metallurgische Prozesstechnik und Metallrecycling, RWTH Aachen University, Aachen, Germany; [c]Jülich Centre for Neutron Science (JCNS-2) and Peter Grünberg Institut (PGI-4), Forschungszentrum Jülich GmbH, Jülich, Germany; [d]Institut für Metallkunde und Metallphysik, RWTH Aachen University, Aachen, Germany; [e]Jülich Centre for Neutron Science (JCNS), Forschungszentrum Jülich GmbH at Heinz Maier-Leibnitz Zentrum (MLZ), Garching, Germany; [f]Mineralogisch-Petrographisches Institut, Universität Hamburg, Hamburg Germany

ABSTRACT

High-pressure devices used in neutron scattering require materials with high strength, low neutron attenuation, and no activation. They should also be non-magnetic. Only very few materials fulfil these criteria. Here, it is reported on the manufacture and properties of the Ni–Cr–Al alloy (57.0 wt-% Ni, 40.0 wt-% Cr, and 3.0 wt-% Al). The casting and heat treatment to obtain the material with the optimal yield strength are described in detail. Synchrotron powder diffraction reveals that phases of the Ni_2Cr, Cr, and Ni_3Al types are present. Aging has no significant effect on their lattice parameters and volume fractions. The alloy has no magnetic order down to at least 1.9 K as evidenced by magnetic measurements and diffraction with polarised neutrons.

ARTICLE HISTORY
Received 5 November 2018
Revised 29 January 2019
Accepted 30 January 2019

KEYWORDS
Neutron scattering; high pressure; magnetism; mechanical properties; Ni–Cr–Al alloy

Introduction

Materials that could be used in high-pressure devices for neutron scattering require not only high strength but also no neutron activation. Their neutron attenuation is to be as low as possible. They should also be non-magnetic at very low temperatures. Among them, the Ni–Cr–Al alloy (NiCrAl), frequently called the *Russian alloy* (40HNU-VI) is considered to be the best [1–6]. It consists of only three elements (57.0 wt-% Ni, 40.0 wt-% Cr, and 3.0 wt-% Al) and is hardened by precipitation. According to the Ni–Cr phase diagram [7,8], Cr dissolves completely in Ni (fcc) at high temperatures for this composition and forms a supersaturated solid solution (Ni, Cr) after quenching. A precipitate of Ni_2Cr and a Ni-bearing Cr forms during annealing at temperatures above 500°C. Al is a precipitation former in nickel-based alloys, which has a strengthening effect.

At room temperature, NiCrAl has a yield strength of about 2.0 GPa, a tensile strength of 2.1 GPa, and an elongation of about 7% [1]. It is possible to reach an ultimate tensile strength of up to about 2.4 GPa, but with an elongation of less than 3% [2]. Eremets [1] has indicated that high-pressure cells could be made of this material when its hardness on the Rockwell C scale (HRC) is in the range 52–56, while the corresponding yield strength is 1.65–1.75 GPa. The material with higher hardness is too brittle. According to his data, the yield strength ($\sigma_{0,2}$) is linearly correlated with the HRC: $\sigma_{0,2} = 0.0264 \times \mathrm{HRC} + 0.2636$. Moreover, small temperature dependence of resistivity and magnetic susceptibility of NiCrAl is beneficial for its applications in neutron scattering [6,9]. Other materials used in pressure cells [3,4] may become activated by neutrons due to the presence of cobalt (e.g. MP35N and maraging steel), have large magnetic susceptibility, or possess low mechanical strength.

NiCrAl has been used in high-pressure technology (especially for clamp cells) in the former Soviet Union for many decades [1,6] but it is not available as a raw material outside the Russian Federation. The pressure cells made of it and currently used in various neutron facilities are designed and manufactured in Russia [10–13]. Also, the whole process to produce the original 40HNU-VI alloy is not exactly known. Uwatoko et al. [9] made an attempt to produce a small quantity of this material containing boron. The Ni–Cr–Al alloy was annealed at 1200°C, followed by water quenching. It was then aged between 400 and 900°C. There are two important issues that Uwatoko et al. [9] did not clarify in their article. They added boron to NiCrAl but they did not indicate which isotope it was. If the added boron is not pure ^{11}B, this material cannot be effectively used for construction of low-attenuation pressure cells for neutron scattering. They also did not mention whether there was any oxidation of the material during the heat treatment and, especially, after water quenching.

Recently, we have started developing various pressure cells for neutron scattering and magnetic measurements. Currently, our diamond anvil cells are made of the Cu–Be alloy [14]. To improve their performance

CONTACT Andrzej Grzechnik grzechnik@xtal.rwth-aachen.de

upon compression, it would be beneficial to use materials with better mechanical properties like, for instance, NiCrAl. Since the 40HNU-VI alloy is not freely available, we have attempted to manufacture it ourselves. Here, we report on our production process and characterisation of NiCrAl using a suite of various experimental techniques.

Methods

The 40HNU-VI alloy was prepared with the composition 57.0 wt-% Ni, 40.0 wt-% Cr and 3.0 wt-% Al to obtain the material with a weight of 50 kg. The Ni pellets (99.95%), Cr granules (99.95%), and Al granules (99.99%) were melted in an Al_2O_3–CaO spinel crucible under an Ar atmosphere (700 mbar of pressure) at 1500°C. Subsequently, the furnace (PVA VSG 100) was switched off and cooled down to room temperature in the Ar atmosphere. The cast rod was about 80 cm in length and 11 cm in diameter.

Several small samples were cut from the rod using spark erosion. Their heat treatment was performed under an Ar flow. The furnace was heated with the rate 300°C/h to various temperatures. After dwelling for 2 hours at the highest temperature, the furnace was shut down and the Ar flow was increased to improve the cooling.

The surface of all samples after the heat treatment was diamond polished to make it smooth and to remove any oxidation products. The Vickers hardness measurements were carried out using the indenter Durimet (Leitz). Nanoindentation tests were performed on a Nanomechanics iNano instrument using a diamond Berkovich indenter calibrated prior to indentation via multiple indents into fused silica [15]. An array of 10×10 indents with the nearest-neighbour distance of 50 µm was made for the measurements on each sample. The unit of the obtained hardness is in GPa and is converted to the Vickers scale (HV) using the relation HV = GPa/9807. The HV → HRC conversion formula is: $\mathrm{HRC} = (100 \times \mathrm{HV} - 14{,}500)/(\mathrm{HV} + 223)$.

Thin samples of the as-cast (raw) material (0.16 mm in thickness) and of the material aged at 750°C (0.11 mm in thickness) were investigated with powder diffraction on the beamline P24 at the synchrotron Petra-III in Hamburg using a marCCD165 detector calibrated with a Si standard ($\lambda = 0.494$ Å). The two-dimensional images were integrated with the program FIT2D to yield intensity versus 2θ diagrams [16]. Le Bail refinements of the diagrams [17] were carried out with the program Jana2006 [18].

Small pieces of the raw sample as well as of the one aged at 750°C (44 and 34 mg, respectively) were studied on the Quantum Design System *Dynacool* with the vibrating sample magnetometer option (VSM). Two measurements were made on each sample. One was to measure the magnetic moment at 0.1 T from 300 K down to 1.9 K with the sweep rate of 2 K/min (the M–T curve). Another one was at 2 K from 7 to −7 T then back to 7 T, with the sweep rate of 100 Oe/sec (the M–H curve).

Polarised neutron diffraction investigations were performed at the cold-neutron spectrometer DNS ($\lambda = 4.2$ Å) in the Heinz Maier-Leibnitz Zentrum (MLZ) in Garching. The neutron transmission measurement was carried out at the neutron reflectometer TREFF ($\lambda = 4.74$ Å) in MLZ (Garching).

A list of samples without annealing at 1200°C and characterised with different methods is shown in Table 1.

Results and discussion

Initially, a heat treatment process similar to that mentioned by Uwatoko et al. [9] was performed, i.e. a small piece was heated at 1200°C for one hour in the air and then water quenched. However, severe oxidation of the sample can be seen afterwards, which is a green layer of Cr_2O_3. Uwatoko et al. [9] did not mention whether there was any oxidation of their material and whether their heat treatment processes were indeed in the air or in an inert atmosphere. Water quenching is necessarily performed in the air, though. To gain a better understanding of the annealing process, another sample (untreated at 1200°C) and the water-quenched one were both aged at 750°C for two hours. The hardness of the sample, measured with the Vickers method, without any heat treatment is 54 HRC. Its hardness decreases to 13 HRC after the annealing at 1200°C and water quenching. It then increases to 51 HRC after aging at 750°C. It is likely that the oxidation influences the hardness of NiCrAl. The hardness of the piece with no annealing at 1200°C and no water quenching increases to 57 HRC after aging at 750°C. On the basis of these hardness tests, a simple aging process without the annealing at 1200°C and water quenching was subsequently used to characterise further the alloy.

The dimensions of the samples changed after the heat treatment. The sample after annealing at 1200°C and water quenching was 0.3–0.8% larger than before. The same sample after additional annealing at 750°C is similar in size to the raw material. The sample after aging at 750°C only is 0.1–0.25% smaller than before the heat treatment.

Four different samples of the as-cast 40HNU-VI alloy (untreated at 1200°C) were aged at 500, 600, 700, and 750°C, respectively, for two hours under the constant Ar flow (Table 1). All the samples were slightly coloured. The colour change can be correlated with the annealing temperature. The higher the temperature, the darker the blue colour can be seen. The average hardness of our samples aged at different temperatures is shown in Figure 1. The tests were performed using both the Vickers and nanoindentation methods.

Table 1. Samples of 40HNU-VI untreated at 1200°C and characterised with various techniques.

Sample	Aging (°C)	Vickers hardness	iNano	M–T curves	M–H curves	Synchrotron diffraction	Neutron scattering	Neutron transmission
#1		✓	✓	✓	✓	✓	✓	✓
#2	500	✓	✓					
#3	600	✓	✓					
#4	700	✓	✓					
#5	750	✓	✓	✓	✓	✓		

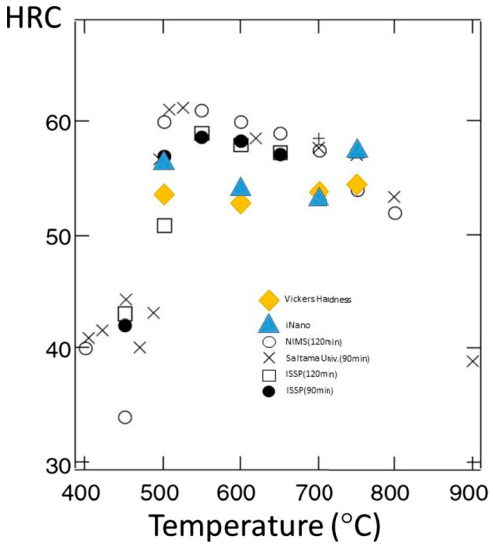

Figure 1. Hardness of the samples aged at different temperatures in this study (yellow diamonds and blue triangles) compared to the hardness of the alloy by Uwatoko et al. [9] determined at other laboratories.

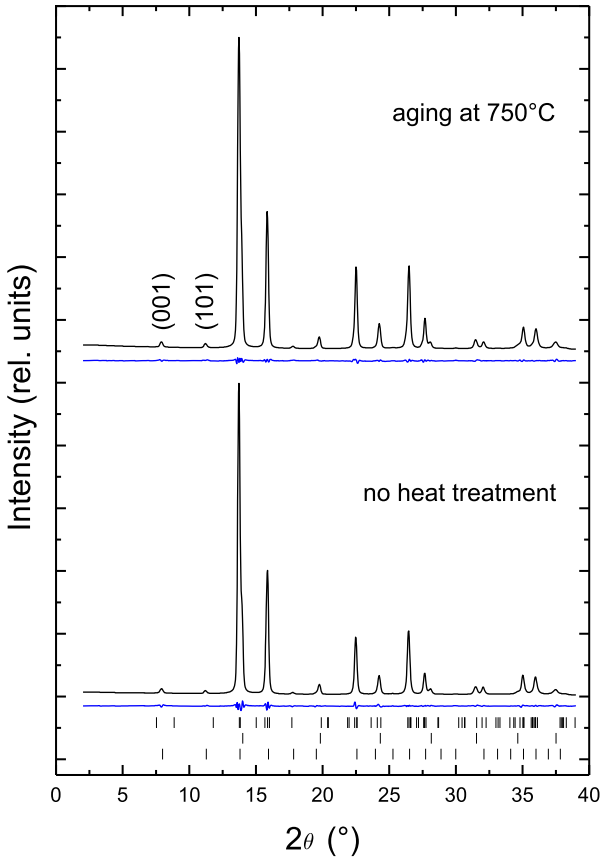

Figure 2. Synchrotron powder diffraction patterns (black curves) of the sample without any heat treatment (#1) and the one aged at 750°C (#5). The ticks indicate the positions of the Bragg reflections due to the Ni_2Cr-, Cr-, and Ni_3Al-type phases (the top, middle, and bottom rows, respectively). The (001) and (101) reflections of the Ni_3Al-type phase are indicated. The difference between the measured and calculated lines using the Le Bail method, assuming the presence of the three phases, is drawn as a blue line for each sample.

As expected, the hardness of our aged alloy is higher than that of the raw sample without any heat treatment. Although, it is slightly lower than that determined on the NiCrAl produced by Uwatoko et al. [9], our data correlate well with the data from other laboratories. Altogether, the hardness of all our samples is within the range HRC = 52–56 that is optimal for manufacturing high-pressure cells [1].

Synchrotron powder diffraction diagrams of two samples produced in this study are shown in Figure 2. They are very similar to each other indicating that aging does not have any substantial effect on the phase composition of the NiCrAl alloy. Phases of the Ni_2Cr ($Immm$, $Z = 2$), Cr ($Im\bar{3}m$, $Z = 2$), and Ni_3Al ($Pm\bar{3}m$, $Z = 1$) types can be identified (Table 2). The presence of the Cr-type phase is documented as a poorly resolved shoulder at about $2\theta = 13.8°$ and a weak reflection at $2\theta = 28.0°$. The estimated volume fraction of the Ni_2Cr phase is about 97.0% in both samples. The fractions of the Cr and Ni_3Al phases are about 0.1 and 2.9%, respectively. The lattice of the orthorhombic Ni_2Cr phase is derived from the fcc one: $a \approx a_{fcc}/\sqrt{2}$, $b \approx 3a_{fcc}/\sqrt{2}$, and $c \approx a_{fcc}$. Aging has hardly any effect also on the lattice parameters of all three phases.

The M–T and M–H curves are shown in Figure 3. For the sample aged at 750°C (sample #5), the magnetisation (M) at 1.9 and 300 K is 0.013 and 0.005 emu/g, respectively. For the sample without any aging (sample #1), the magnetisation is 0.0096 and 0.0035 emu/g at 1.9 and 300 K, respectively. This is consistent with the results by Sadykov [6], which show that the magnetisation is 0.013 emu/g at very low temperatures and 0.0035 emu/g at 300 K. It can be seen in the M–T curves that the magnetisation is nearly constant from 300 K to 25 K (Figure 3). It then suddenly increases at lower temperatures. The magnetisation is zero when there is no external field. It means that the material is paramagnetic.

Diffraction measurements on the non-heat-treated sample (#1) using polarised neutrons were performed at the instrument DNS (MLZ, Garching). The results

Table 2. Lattice parameters of the phases observed in the synchrotron powder diffraction patterns of the sample with no aging and of the one aged at 750°C.

a (Å)	*b* (Å)	*c* (Å)	
No aging (*sample #1*)			
Ni_2Cr type	2.5523(5)	7.602(1)	3.5644(5)
Cr type	2.8801(2)		
Ni_3Al type	3.5811(2)		
750°C (*sample #5*)			
Ni_2Cr type	2.5559(3)	7.578(1)	3.5666(4)
Cr type	2.8808(2)		
Ni_3Al type	3.5773(1)		

show (Figure 4) that the NiCrAl alloy is magnetically disordered at 3.7 K because magnetic incoherent contribution to neutron scattering is not observed. Two nuclear coherent scattering peaks at 1.75 and 2.49 $Å^{-1}$ (d-spacing of 3.59 and 2.52 Å, respectively) correspond to the first two Bragg (001) and (101) reflections of the Ni_3Al-type phase detected in synchrotron powder diffraction diagrams shown in Figure 2.

Neutron transmission of the raw sample (#1, thickness of 6 mm, density of 7.6 g/cm^3) measured using the neutron reflectometer TREFF at MLZ (Garching) is 47.5%. Assuming the attenuation formula as $I/I_0 = \exp(-\mu^* d)$, the transmission of the sample with the same thickness but made of the CuBe alloy could be compared to this value. The attenuation coefficient of CuBe is wavelength dependent: $\mu_{CuBe} = 0.1611\lambda + 0.041$ (cm^{-1}) [19]. Accordingly, the sample made of CuBe would have a transmission of 61.7% at a wavelength of 4.74 Å. Hence, the Ni–Cr–Al alloy transmits fewer neutrons than CuBe. On the other hand, its mechanical and magnetic properties are far superior to those of CuBe.

Conclusions

The crystallographic and magnetic data on the investigated Ni–Cr–Al alloy (40HNU-VI) obtained with synchrotron and neutron scattering, respectively, are presented here for the first time. The following conclusions can be drawn from the present work:

(1) the Ni–Cr–Al alloy can be produced using a method that precludes oxidation and does not require boron as an additive;
(2) it has optimal mechanical properties for neutron scattering at high pressures using diamond anvil and clamp cells;

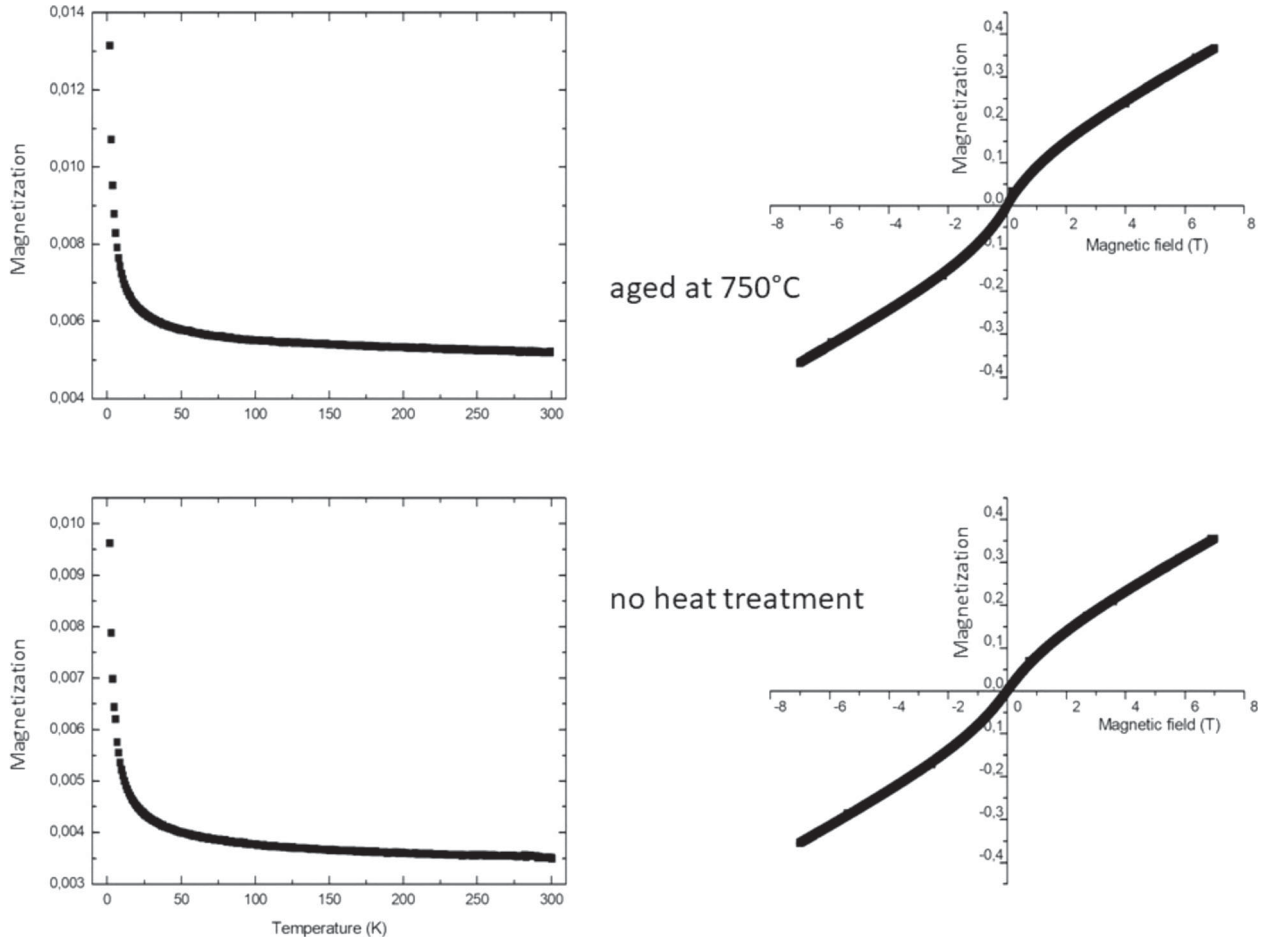

Figure 3. M–T and M–H curves for the sample aged at 750°C (#5) and for the sample without any heat treatment (#1).

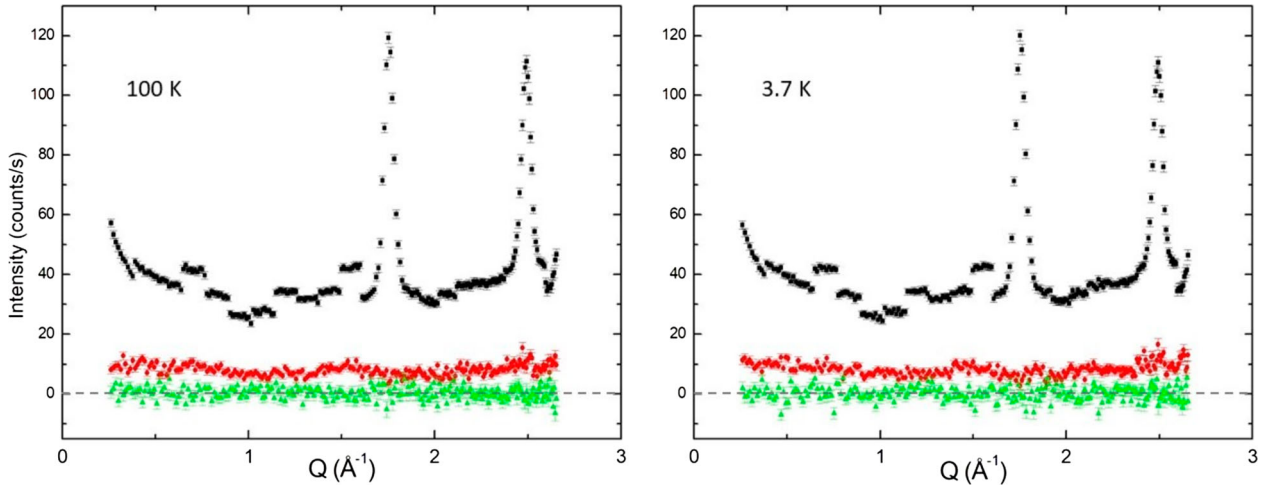

Figure 4. Nuclear coherent (black symbols), magnetic (green symbols), and spin incoherent (red symbols) contributions to scattering of the heat untreated sample (#1) at 100 K (left) and 3.7 K (right) measured at the instrument DNS (MLZ, Garching).

(3) the Ni_2Cr-, Cr- and Ni_3Al-type phases are present in the produced alloy as identified by synchrotron powder diffraction. Aging has hardly any effect on the lattice parameters and volume fractions of all three phases;
(4) the alloy was found to be paramagnetic. Diffraction measurements using polarised neutrons clearly show that the alloy is magnetically disordered at very low temperatures since magnetic incoherent contribution to neutron scattering is not detectable.

Acknowledgements

We thank Sebastian Benz and Karen Friese for discussions as well as Peter Link for his help with the measurement at TREFF. Micha Hölzle assisted us with the sample machining.

Disclosure statement

No potential conflict of interest was reported by the authors.

Funding

This work is supported by the project 05K16PA3 from the Bundesministerium für Bildung und Forschung (BMBF). Nour Maraytta acknowledges support from the Palestinian-German Science Bridge (PGSB).

ORCID

Bernd Friedrich http://orcid.org/0000-0002-2934-2034
Jörg Perßon http://orcid.org/0000-0001-5664-9341
James S. K.-L. Gibson http://orcid.org/0000-0002-2274-4057

References

[1] Eremets MI. High pressure experimental methods. Oxford: Oxford University Press; 1996.
[2] Walker IR. Nonmagnetic piston-cylinder pressure cell for use at 35 kbar and above. Rev Sci Instr. 1999;70(8):3402.
[3] Walker IR. Considerations on the selection of alloys for use in pressure cells at low temperatures. Cryogenics (Guildf). 2005;45(2):87–108.
[4] Palmer A, Silevitch DM, Feng Y, et al. Sub-Kelvin magnetic and electrical measurements in a diamond anvil cell with in situ tenability. Rev Sci Instr. 2015;86(9):093901.
[5] Klotz S. Techniques in high pressure neutron scattering. Boca Raton: CRC Press; 2013.
[6] Sadykov RA. Private communication (2016).
[7] ASM handbook. Vol. 3, Alloy phase diagrams. ASM; 1992.
[8] Wang Y, Cacciamani G. Thermodynamic modeling of the Al-Cr-Ni system over the entire composition and temperature range. J Alloys Comp. 2016;688:422–435.
[9] Uwatoko Y, Todo S, Ueda K, et al. Material properties of Ni-Cr-Al alloy and design of a 4 GPa class non-magnetic high-pressure cell. J Phys Condens Matter. 2002;14:11291–11296.
[10] Bezaeva NS, Chareevd DA, Rochettee P, et al. Magnetic characterization of non-ideal single-domain monoclinic pyrrhotite and its demagnetization under hydrostatic pressure up to 2 GPa with implications for impact demagnetization. Phys Earth Planet Inter. 2016;257:79–90.
[11] Kolesnikov AI, Podlesnyak A, Sadykov RA, et al. Pressure effect on hydrogen tunneling and vibrational spectrum in α-Mn. Phys Rev B. 2016;94:134301.
[12] Sadykov RA, Th S, Podlesnyak A, et al. High-pressure cells for study of condensed matter by diffraction and inelastic neutron scattering at low temperatures and in strong magnetic fields. J Phys Conf Ser. 2017;941:012082.
[13] Sadykov R, Pappas C, Bannenberg LJ, et al. 1.5 GPa compact double-wall clamp cell for SANS and NSE studies at low temperatures and high magnetic fields. J Neutron Res. 2018;20:25–33.
[14] Grzechnik A, Meven M, Friese K. Single-crystal neutron diffraction in diamond anvil cells with hot neutrons. J Appl Cryst. 2018;51:351–356.
[15] Oliver WC, Pharr GM. An improved technique for determining hardness and elastic modulus using load and displacement sensing indentation experiments. J Mater Res. 1992;7(6):1564–1583.

[16] Hammersley AP, Svensson SO, Hanfland M, et al. Two-dimensional detector software: from real detector to idealised image or two-theta scan. High Press Res. 1996;14(4–6):235–248.
[17] Le Bail A. Whole powder pattern decomposition methods and applications: a retrospection. Powder Diffr. 2005;20:316–326.
[18] Petříček V, Dušek M, Palatinus L. Crystallographic computing system JANA2006: general features. Z Kristallogr. 2014;229(5):345–352.
[19] Binns J, Kamenev KV, McIntyre GJ, et al. Use of a miniature diamond-anvil cell in high-pressure single-crystal neutron Laue diffraction. IUCrJ. 2016;3:168–179.